

Modeling Rainfall Intensity-Duration-Frequency (IDF) and Establishing Climate Change Existence in Uyo-Nigeria Using Non-Stationary Approach

Masi G. Sam¹, Ify L. Nwaogazie^{1*}, Chiedozie Ikebude¹, Ubong J. Inyang², Jonathan O. Irokwe¹

¹Department of Civil and Environmental Engineering, University of Port Harcourt, Port Harcourt, Nigeria

²Center for Occupational Health, Safety & Environment, University of Port Harcourt, Port Harcourt, Nigeria

Email: *ifynwaogazie@yahoo.com

How to cite this paper: Sam, M.G., Nwaogazie, I.L., Ikebude, C., Inyang, U.J. and Irokwe, J.O. (2023) Modeling Rainfall Intensity-Duration-Frequency (IDF) and Establishing Climate Change Existence in Uyo-Nigeria Using Non-Stationary Approach. *Journal of Water Resource and Protection*, 15, 194-214.
<https://doi.org/10.4236/jwarp.2023.155012>

Received: March 21, 2023

Accepted: May 16, 2023

Published: May 19, 2023

Copyright © 2023 by author(s) and Scientific Research Publishing Inc.
This work is licensed under the Creative Commons Attribution International License (CC BY 4.0).

<http://creativecommons.org/licenses/by/4.0/>



Open Access

Abstract

This study aims at establishing if climate change exists in the Niger Delta environment using non-stationary rainfall Intensity-Duration-Frequency (IDF) modelling incorporating time-variant parameters. To compute the intensity levels, the open-access R-studio software was used based on the General Extreme Value (GEV) distribution function. Among the four linear parameter models adopted for integrating time as a covariate, the fourth linear model incorporating scale and location with the shape function constant produced the least corrected Akaike Information Criteria (AICc), varying between 306.191 to 101.497 for 15 and 1440 minutes, respectively, selected for calibration of the GEV distribution equation. The non-stationary intensities yielded higher values above those of stationary models, proving that the assumption of stationary IDF models underestimated extreme events. The difference of 13.71 mm/hr (22.71%) to 14.26 mm/hr (17.0%) intensities implies an underestimation of the peak flood from a stationary IDF curve. The statistical difference at a 95% confidence level between stationary and non-stationary models was significant, confirming evidence of climatic change influenced by time-variant parameters. Consequently, emphasis should be on applying shorter-duration storms for design purposes occurring with higher intensities to help reduce the flood risk and resultant infrastructural failures.

Keywords

Precipitation, Annual Maximum Series, Stationary, Non-Stationary, Intensity-Duration-Frequency Models, Trends

1. Introduction

It is common knowledge that the designs of both hydrologic and hydraulic infrastructures are dependent on the prediction of rainfall Intensities using IDF models and the corresponding runoff values. The stationary assumption of IDF models that extremes will not significantly vary over time has been popularly used. The construction of stationary IDF relationships is based on at-site frequency analysis of rainfall data considered separately for different durations. These relationships depend on many assumptions which render them inaccurate and unreliable because a large number of parameters that are not time-dependent are required. The inclusion of some required parameters gave rise to parametric IDF models which have many de-merits. Non-stationary IDF modelling, however, utilizes dynamic data series in which the descriptive statistics of the sample mean, variance and covariance change over time. Neglecting to incorporate non-stationary concepts in hydrological modelling will probably lead to inaccurate results [1]. A check on the trend of the rainfall data is required to ascertain the presence of dynamic sequential behaviour. Where a significant trend is found, the location parameters will be computed based on the non-stationary assumption. This allows for the evaluation of rainfall quantities that are consistent with the ideal characteristics of the measured rainfall extremes. Most recent studies embarked upon focused on the development of IDF curves with consideration of the non-stationary concept [1] [2] [3] [4]. [2] in their study proposed a scaling method for the rainfall IDF relationship and proved that rainfall follows a simple scaling process that is more efficient with more accurate estimates in non-stationary IDF modelling than that from the stationary approach.

[5] in their study outlined a framework for evaluating climate change impacts on natural and man-made infrastructure using bias-corrected multi-model simulations of historical and projected precipitation extremes. The method derived changes in rainfall IDF curves and their uncertainty bounds using a non-stationary model by integrating Bayesian Inference. [1] in their investigation of non-stationary IDF curves integrating information relating to teleconnections and climate change presented results that showed that the non-stationary framework for IDF modelling gives a better fit to the sample data than the stationary method. Also, [6] worked on the impacts of spatial heterogeneity and temporal non-stationary on IDF estimates—A case study in a Mountainous California-Nevada Watershed. The result presented indicated the existence of strong heterogeneity and variability in IDF estimates with high-resolution simulation data with discrepancies in spatial variability that supports the use of an ensemble in non-stationary modelling.

This study is focused on the development of 24-hourly Annual Maximum Series (AMS) non-stationary rainfall Intensity-Duration-Frequency (IDF) model for a deltaic environment using a statistical approach for fitting General Extreme Value (GEV) distribution via the maximum likelihood method to establish climate change existence. The flowchart in **Figure 1** shows the summary of the basic

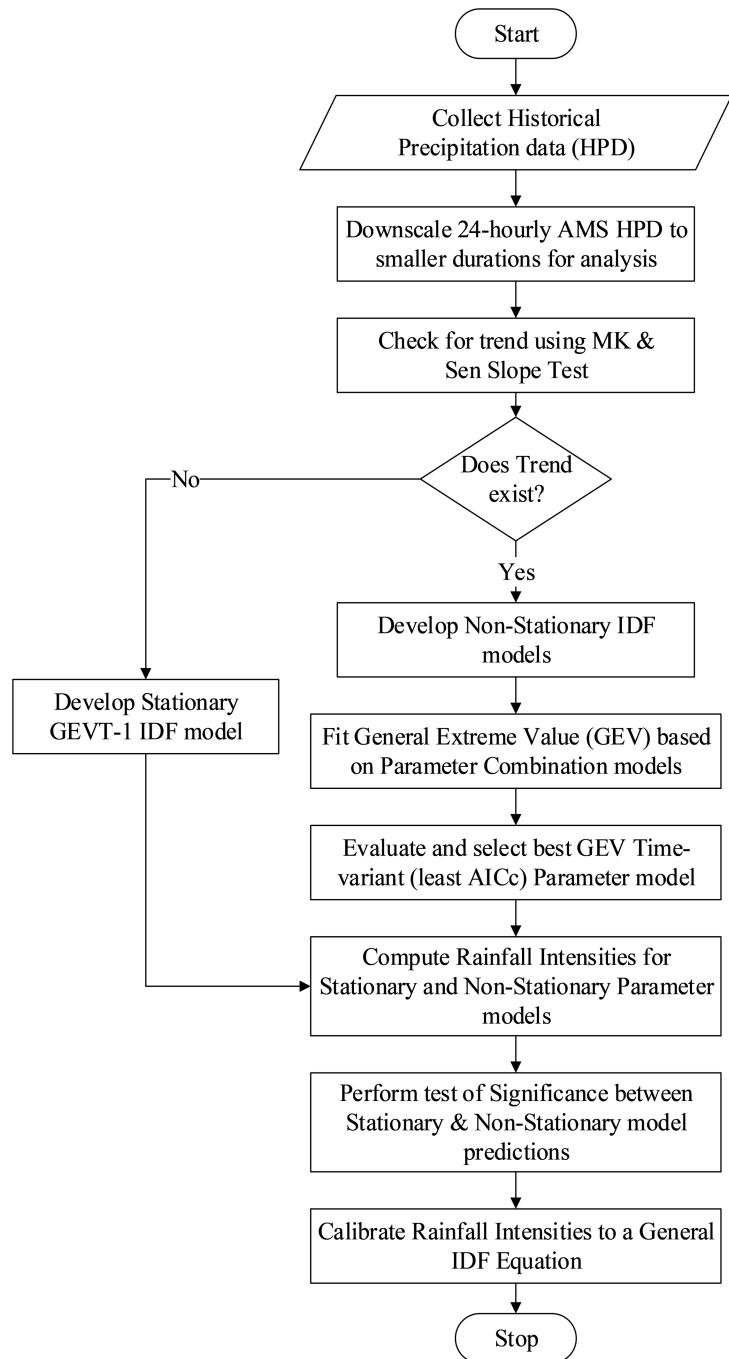


Figure 1. Flow chart for development of 24-hourly rainfall non-stationary IDF models.

steps to follow for the development of a 24-hourly GEV distribution function-based non-stationary model and its stationary-based parameter model counterpart.

2. Materials and Methods

2.1. Study Area

The study area, Uyo metropolis is located in Akwa Ibom State, in South-Eastern Nigeria. The GPS coordinates for the location of Uyo are between Latitudes:

4°52'N - 5°7'N and Longitudes: 7°50'E - 8°0'E with elevation above sea level as 45 m (see **Figure 2** sourced and modified from [7]). The topography of the area is characterized by undulating sandy plain terrain that is well-drained to the Atlantic Ocean at the southern end. The mean daily maximum and minimum temperature of Uyo is 34°C and 23°C, respectively; with average humidity of 72% mostly during January. The range of annual rainfall varies from 1599.5 mm (1983) to 3855.5 mm (1977). The value of mean annual rainfall is 2466.6 mm with higher intensities occurring from April to October, with prolonged rainstorms exhibited [8].

2.2. Data Collection

The historical precipitation records of the study area between 1986 and 2015 (30 years) were collected from the Meteorological gauge station of the Department of Oceanography and Regional Planning of the University of Uyo. The rainfall records collected were sorted and recorded as rainfall amounts in mm against corresponding durations in minutes. Extraction of the daily (24-hourly) annual maximum series for the rest of the 30 years were thereafter obtained first on monthly basis for each year out of which the annual maximum daily rainfall amount was extracted.

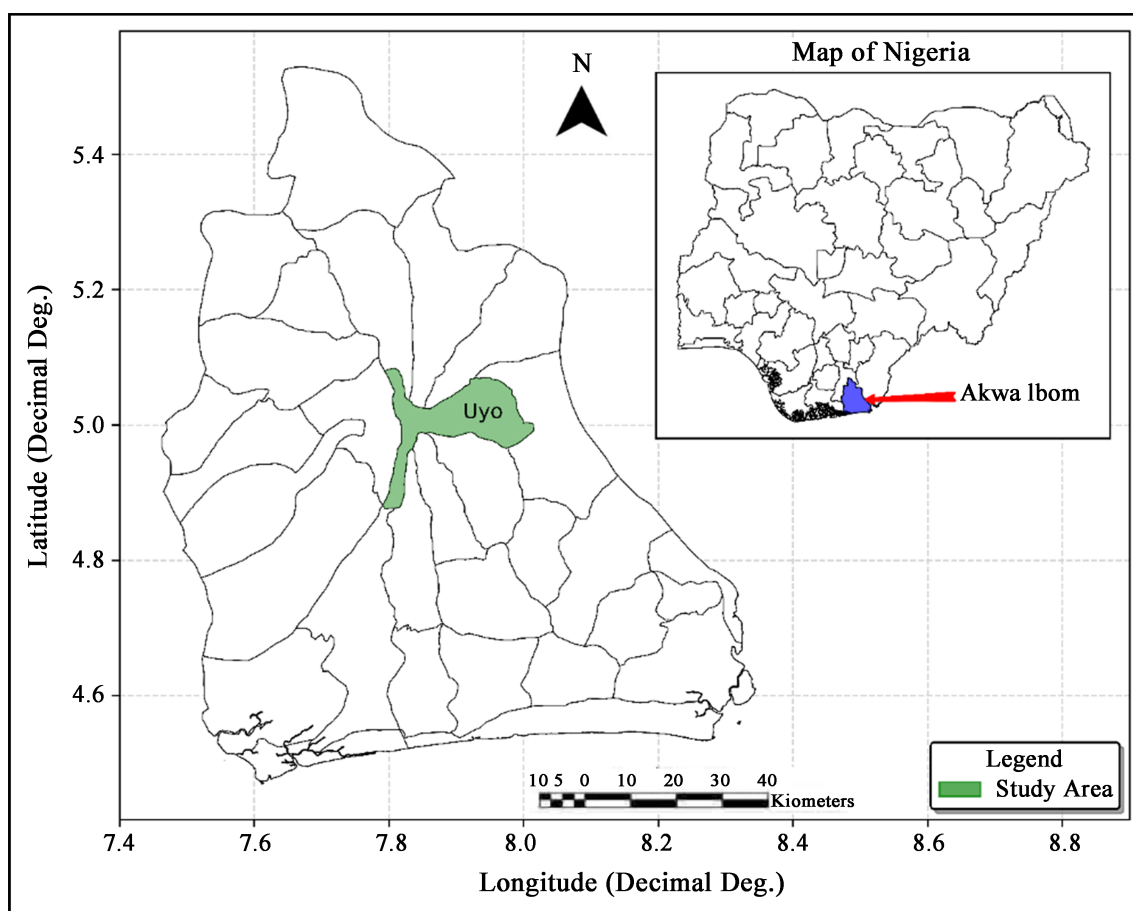


Figure 2. Map of Akwa Ibom State in Nigeria showing study area—Uyo.

2.3. Disaggregation of Short Duration Rainfall

The 30-year 24-hourly AMS data sorted out were downscaled into shorter durations of 15 to 720 minutes at increments of 15 minutes. The reduction of sorted AMS into a time scale of shorter values of less than 24 hours was achieved using scaling relationships in Equation (1) originally proposed by [9] to the Indian Meteorological Department (IMD),

$$R_t = R_{24} \left(\frac{t}{24} \right)^n \quad (1)$$

And the Modified Chowdhury Indian Meteorological Department (MCIMD) method given in Equation (2):

$$R_t = R_{24} \left(\frac{t}{24} \right)^n + C \quad (2)$$

$$\text{with, } I = R_t/t \quad (3)$$

where: R_t is the required rainfall depth in mm for durations less than 24 hours, R_{24} is the daily rainfall depth in mm, t is the required duration in hours and n is an exponential constant = 1/3. However, the corresponding values of disaggregated rainfall intensities in **Table 1** were calculated based on the MCIMD [10] from Equation (2). Where n and C are calibrated constants. The MCIMD method is a modified version of Equation (1) where the basis for the Chowdhury model also remains the use of 24-hour event rainfall depth R_{24} , with I = rainfall intensity in mm/hr.

2.4. Calibration of MCIMD Rainfall Downscaling Methods

The calibration of the MCIMD formula was obtained using the Excel optimization solver tool. The existing rainfall general GEVT-1 IDF equation obtained based on the Conventional Annual Maximum Series (CAMS) method for the study area published in [11] was adopted for generation of the control experiment or actual observed rainfall intensity data. These observed rainfall intensities were compared with rainfall intensities downscaled using the original IMD method in Equation (1). The sum of squares of their differences was obtained and optimization was carried out by minimizing the sum of square differences [12].

The optimizing functions were applied to obtain the best-fit values for the exponent (n) and constant (C) for the MCIMD. Thus, the calibrated MCIMD downscaling model used was obtained based on the GEVT-1 probability distribution function IDF model type. Thus, the corresponding values of disaggregated rainfall intensities for this study were calculated based on the calibrated MCIMD Equation (4):

$$P_t = P_{24} \left(\frac{t}{24} \right)^{0.252} + 6.0 \quad (4)$$

The details of the calibration process can be found in our earlier publication

[13]. The calibrated Equation (4) can be applied for rainfall intensities down-scaling within the study region or catchment area. However, for other areas it will be ideal to use local rainfall measurement records to effect the calibration of Equation (2) due to the influence of local physiographic parameters.

2.5. Check for Climatic Trends in Collected Data

Testing for non-stationary signals is required on the historical rainfall intensity data documented in [14]. The rank-based non-parametric revised Mann-Kendall method was applied to the data to detect statistically significant trends [15] [16] [17]. Also, Theil-Sen's non-parametric method was applied to estimate the magnitude of trends in the time series data [16] [17].

2.6. Generalized Extreme Value (GEV) Distribution in Non-Stationary IDF Modeling

Non-stationary models are usually better fitted on data sequences of specific durations where a single model with a separate functional relation with the return period and rainfall duration could be used. The Generalized Extreme Value (GEV) distribution is introduced as the time-dependent function in the general IDF relationship [3]. The GEV distribution is based on the limit theorems for block maxima or annual maxima and consists of continuous probability distributions that are a combination of the three asymptotic extreme value distributions into a single one—Gumbel (EV1), Fréchet (EV2) and Weibull (EV3). The GEV distribution is adaptable for the modelling of different behaviour of extremes with three distribution parameters: location, scale and shape [18]. The location parameter describes the shift of distribution in each direction on the horizontal axis. The scale parameter describes how spread out the distribution is, and defines where the bulk of the distribution lies. As the scale parameter increases, the distribution becomes more spread out. The shape parameter affects the characteristics of the distribution tail. The shape parameter is derived from skewness, as it represents where most of the data lies, which creates the tail(s) of the distribution. The value of shape parameter $\xi = 0$, indicates the light tale EV1 (Gumbel) distribution. The value of $\xi > 0$ indicates EV2 (Fréchet), and $\xi < 0$ is EV3 (Weibull). The Fréchet type has a longer (heavy) upper tail than the Gumbel distribution and the Weibull has a short tail [19] [20]. The standard Cumulative Distribution Function (CDF) of the GEV as expressed by [21] can be presented in the form of Equation (5):

$$F(x) = \exp \left[- \left(1 + \xi(t) \frac{x - \mu(t)}{\sigma(t)} \right)^{-1/\xi(t)} \right] \quad \text{for } \xi \neq 0 \quad (5)$$

where: $F(x)$ = Cumulative Distribution Function, ξ = shape parameter, μ = mean and σ = standard deviation.

The statistical procedure used for estimating the distribution parameters is the maximum likelihood estimator; because the method can be easily extended to the

non-stationary evaluation. Non-stationarity is introduced by expressing one or more of the parameters of the GEV as a function of time, as $\mu(t)$, $\sigma(t)$ and $\xi(t)$, $t = 1, 2, \dots$ [21] [22].

2.7. Evaluation of Time-Variant Parameters

The extreme value theory of stationary random series assumes that statistical properties of extremes such as distribution parameters $\theta = (\mu, \sigma, \xi)$ are independent of time [23]. In contrast, in a non-stationary process, the parameters of the fundamental distribution function are time-dependent and have time-varying properties [24]. In order to represent a dynamic distribution, the location and scale parameters are assumed to be linear functions of time to account for non-stationarity, with the shape parameter kept constant [4] [18] [23] [25] [26]. Thus, the time-varying covariates are incorporated into GEV location (GEV-I), and into both location and scale parameters (GEV-II) respectively, thereby describing trends as a linear function of time in years as follows:

$$\mu(t) = \mu_1 t + \mu_o \tag{6}$$

$$\sigma(t) = \sigma_1 t + \sigma_o \tag{7}$$

Because the scale parameter must remain positive all through for a log link function is used in the modelling [27]:

$$\ln \sigma(t) = \sigma_1 t + \sigma_o \tag{8}$$

$$\text{or, } \sigma(t) = \exp(\sigma_1 t + \sigma_o) \tag{9}$$

where: t is the time (in years), and $\tau = (\mu_1, \mu_o, \sigma_1, \sigma_o, \xi)$ are the regression parameters.

This study considered four different model combinations of the GEV parameters by assuming a case of a linear trend for location and a linear trend for scale parameters and their different combinations presented in **Table 1** [28]. Given a typical rainfall duration of values $X = X_1, X_2, \dots, X_n$, for n years of the annual maximum time series. The log-likelihood for the Stationary given the condition of Equation (10), is expressed as written in Equation (11):

$$\text{For } \xi \neq 0 \text{ and } 1 + \xi \left(\frac{x_i - \mu}{\sigma} \right) > 0 \tag{10}$$

$$\begin{aligned} \log L(\mu, \sigma, \xi | X) = & -n \log \sigma - \left(1 + \frac{1}{\xi} \right) \sum_{i=1}^n \log \left[1 + \xi \left(\frac{x_i - \mu}{\sigma} \right) \right] \\ & - \sum_{i=1}^n \left[1 + \xi \left(\frac{x_i - \mu}{\sigma} \right) \right]^{-1/\xi} \end{aligned} \tag{11}$$

where: the Maximum Likelihood Estimates (MLEs) are the parameter values that maximize the likelihood function so that instead of maximization, the minimization of the negative log-likelihood function becomes more ideal. This formulation easily allows for the extension to the non-stationary case, in which the parameters of the GEV distribution depend on time, t [22] [29]. To obtain the

Table 1. GEV linear model types selected.

Model Type	Parameter Combination	Remark
GEV _t -0	$\mu(t) = \mu$ $\sigma(t) = \sigma$ $\xi(t) = \xi$	Stationary parameter model
GEV _t -I	$\mu(t) = \mu_o + \mu_1 t$ $\sigma(t) = \sigma$ $\xi(t) = \xi$	Non-stationary parameter model
GEV _t -II	$\mu(t) = \mu$ $\sigma(t) = \sigma_o + \sigma_1 t$ $\xi(t) = \xi$	Non-stationary parameter model
GEV _t -III	$\mu(t) = \mu_o + \mu_1 t$ $\sigma(t) = \sigma_o + \sigma_1 t$ $\xi(t) = \xi$	Non-stationary parameter model

parameters of extreme distributions as the GEV by minimizing the negative log-likelihood function, are evaluated using the iterative numerical procedure.

2.8. Selection of the Best GEV Model

After non-stationary models' development, it is important to identify which model better represents the original data. To select the best model, we use the corrected Akaike Information Criteria (AICc), which penalizes the minimized negative log-likelihood for the number of parameters estimated [22]. According to [30], AICc is recommended in practical applications because it outperforms the original AIC and helps to avoid over-fitting the data. From a collection of nested candidate models, AIC selects the model that minimizes the quantity:

$$\text{AIC}(k) = 2 * \text{nllh}(k) + 2k \quad (12)$$

where: $\text{nllh} = -\log L$, is the minimized negative log-likelihood function; and k is the number of parameters of the specific model. For a candidate model with k parameters, which has a sample size of n , then the AICc of the model is as follows:

$$\text{AIC}(k) = \text{AIC}(k) + \frac{2k(k+1)}{n-k-1} \quad (13)$$

The rescaled form of AICc, Δi is used to rank the GEV models as follows:

$$\Delta i = \text{AICc} - \min(\text{AICc}) \quad (14)$$

where: $\min(\text{AICc})$ is the smallest AICc among all the models. The model which has Δi value zero is the best model and the models having $\Delta i \leq 2$ are considera-

ble reasonable good choices.

2.9. Development of Non-Stationary Intensity Duration Frequency Curves

The model parameters are used to estimate the non-stationary precipitation intensities or equivalent return levels. [31] showed that by using the GEV distribution, the return periods and return levels of extremes in Equations (15) and (16) are determined by expressing return levels as a function of the return period T :

$$T = \frac{1}{1-P} \quad (15)$$

where: p is the non-exceedance probability of occurrence in a given year, assumed constant under stationary.

The rainfall Intensity Duration Frequency curve for Uyo city was developed with the aid of R-studio software. The extreme values are computed based on the Generalized Extreme Value distribution which is a combination of the Gumbel, Frechet and Weibull distributions. The Cumulative Distribution Function (CDF) of GEV is given by Equation (5) and inverting the CDF will result to Equation (16) for computation of the Stationary rainfall extreme intensity values [3] [21]:

$$x_T = \mu(t) - \frac{\sigma(t)}{\xi(t)} \left[1 - \left\{ -\ln \left(1 - \frac{1}{T} \right)^{-\xi(t)} \right\} \right] \quad \text{for } \xi \neq 0 \quad (16)$$

However, the model parameters estimated on the conditions of non-stationarity in the behavioural parameter extremes can then be used to estimate the non-stationary return level or rainfall intensity based on Equation (17):

$$\bar{x} = Q_K(\mu_{t_1}, \mu_{t_2}, \dots, \mu_m), (\mu(t) = \mu_1 t + \mu_0)$$

$$x_T = \left[\left(-\frac{1}{\ln P} \right)^\xi - 1 \right] \times \frac{\sigma}{\xi} + \bar{\mu}, (\xi \neq 0) \quad (17)$$

where: x_T = rainfall intensity exceedance value, and T = return period. Also, the return levels are similarly translated into intensities for each return period and duration, with IDF curves plotted. The R-Studio software package was similarly applied for the computation of the storm intensities

2.10. Test for Significant Difference between Stationary versus Best Non-Stationary IDF Predicted Rainfall Intensities

The statistical significance of the best non-stationary model against the stationary one can be provided by the Wilcoxon signed rank sum (non-parametric) test, by assessing the statistically significant difference in their computed rainfall intensities. The test is used to evaluate if there exists a significant difference between the selected best parameter non-stationary models with that of the stationary model. The null hypothesis is accepted if the critical value that corresponds to alpha, $\alpha = 0.05$ at reduced sample size, n , is greater than the computed statistic value. The statistical significance of the best non-stationary model when com-

pared against the stationary model can be measured from the p-value of the Wilcoxon signed rank statistic test at 5% level of significance [32].

3. Results and Discussion

3.1. Analysis of Results

3.1.1. Downscaling 24-Hourly AMS Data into Shorter Durations

Thirty years of Historical Precipitation Data (HPD) were collected and sorted out into 24-hourly Annual Maximum Series (AMS) for each year. The calibrated MCIMD Equation (6) was thereafter used to disaggregate the 24-hourly AMS into shorter durations of 0.25, 0.56, and 12 hours as shown in **Table 2**. The IMD downscaling method could also be used, however, the MCIMD method produced higher and improved precipitation intensities.

3.1.2. Generalized Extreme Value (GEV) Distribution Fitted Non-Stationary IDF Curves

The rainfall IDF curves for Uyo city were developed with the aid of open-access software provided by [33]. The extreme values were computed based on the GEV distribution which has the combination of Gumbel, Frechet and Weibull distributions. The Cumulative Distribution Function (CDF) of GEV given in Equation (5) was the basis for the derivation of the log-likelihood function. Thus, the formulation of the expression enabled the optimization of the log-likelihood function which allowed for its extension to the non-stationary modelling, in which the parameters of the GEV distribution depend on time t . The inverted GEV equation resulted in Equation (16) used for the computation of the rainfall intensity values. However, to obtain the parameters of the external distribution of the GEV, this was actualized by minimizing the negative likelihood function through the iterative numerical method. Subsequently, non-stationarity was introduced by expressing one or more of the parameters of the GEV as a function of time (see **Table 2**).

The condition to conduct non-stationary IDF modelling is the establishment of a trend in the time series data constructed for any modelling. To realize this objective, a statistical procedure utilized was the non-parametric Mann-Kendall (MK) test which produced a positive trend. **Table 3** shows the performances of the different statistical parameters expressed as a function of time and their values. The best linear behavioural model was selected based on the corrected Akaike Information Criteria (AICc) indicated in Equation (19). The model that had the lowest AICc is the model that best represented the time series data. The various rainfall intensity value was computed for the non-stationary IDF curves based on the best model selected. From **Table 3**, GEVt-III had the lowest AICc, from which the rainfall intensities were estimated. The result of the rainfall intensity computed for both the stationary and Non-stationary models using Equation (16) are presented in **Table 4** and **Table 5**, respectively. **Figure 3** indicates the graphical plots of GEV distribution fitted non-stationary versus stationary IDF curves on same graph paper for different return periods, while **Figure 4**

shows the case of GEV distribution fitted non-stationary versus Stationary IDF curves plotted on the same graph paper for different durations for Uyo, respectively.

Table 2. Downscaled rainfall intensity using MCIMD formula for Uyo.

Year No.	0.25 hr	0.5 hr	0.75 hr	1 hr	2 hrs	6 hrs	12 hrs	24 hrs
1	167.6 [±]	97.5	71.1	56.9	33.3	14.3	8.4	5.0
2	139.9	81.0	58.9	47.1	27.5	11.8	6.9	4.1
3	200.3	117.0	85.5	68.5	40.2	17.4	10.2	6.1
4	144.8	83.9	61.1	48.8	28.5	12.2	7.2	4.2
5	134.5	77.8	56.6	45.2	26.3	11.3	6.6	3.9
6	164.9	95.9	70.0	56.0	32.8	14.1	8.3	4.9
7	129.6	74.9	54.4	43.4	25.3	10.8	6.3	3.7
8	176.3	102.7	75.0	60.0	35.2	15.1	8.9	5.3
9	187.6	109.4	79.9	64.0	37.5	16.2	9.5	5.6
10	212.0	124.0	90.7	72.7	42.7	18.5	10.9	6.4
11	193.4	112.9	82.5	66.1	38.8	16.7	9.9	5.8
12	161.3	93.7	68.3	54.7	32.0	13.7	8.1	4.8
13	172.7	100.5	73.4	58.7	34.4	14.8	8.7	5.1
14	149.9	86.9	63.3	50.6	29.6	12.7	7.5	4.4
15	174.1	101.3	74.0	59.2	34.7	14.9	8.8	5.2
16	121.2	69.9	50.8	40.5	23.5	10.0	5.9	3.5
17	134.5	77.8	56.6	45.2	26.3	11.3	6.6	3.9
18	200.3	117.0	85.5	68.5	40.2	17.4	10.2	6.1
19	200.3	117.0	85.5	68.5	40.2	17.4	10.2	6.1
20	212.0	124.0	90.7	72.7	42.7	18.5	10.9	6.4
21	202.7	118.4	86.6	69.3	40.7	17.6	10.4	6.1
22	172.7	100.5	73.4	58.7	34.4	14.8	8.7	5.1
23	172.7	100.5	73.4	58.7	34.4	14.8	8.7	5.1
24	148.2	86.0	62.6	50.0	29.2	12.5	7.4	4.3
25	208.7	122.0	89.2	71.5	42.0	18.1	10.7	6.3
26	251.9	147.7	108.2	86.8	51.1	22.2	13.1	7.8
27	198.1	115.7	84.5	67.7	39.8	17.2	10.1	6.0
28	232.3	136.0	99.6	79.9	47.0	20.3	12.0	7.1
29	326.5	192.1	141.0	113.3	66.9	29.1	17.2	10.2
30	273.8	160.8	117.8	94.6	55.7	24.2	14.3	8.5

Note: [±]Dis-segregated rainfall intensities (mm/hr).

Table 3. Performance of GEV parameters evaluated for non-stationary and stationary models.

Time (mins)	Models	Location Parameter	Scale	Shape Parameter	AIC	AICc
15	GEV _t -0	165.13	33.101	0.0367	311.938	312.861
	GEV _t -I	130.580 + 2.606t	32.203	-0.1354	305.853	307.453
	GEV _t -II	159.0525	14.289 + 1.510t	-0.2245	308.123	309.723
	GEV _t -III	140.637 + 1.981t	17.285 + 0.926t	-0.1848	303.691	306.191
30	GEV _t -0	96.026	19.703	0.0374	280.838	281.761
	GEV _t -I	75.475 + 1.551t	19.171	-0.135	274.754	276.354
	GEV _t -II	92.405	8.494 + 0.900t	-0.2243	277.038	278.638
	GEV _t -III	81.477 + 1.177t	10.286 + 0.551t	-0.1842	272.602	275.102
45	GEV _t -0	70.045	14.548	0.0373	262.63	263.553
	GEV _t -I	54.888 + 1.145t	14.16	-0.1351	256.534	258.134
	GEV _t -II	67.37	6.276 + 0.665t	-0.225	258.843	260.443
	GEV _t -III	59.282 + 0.871t	7.593 + 0.407t	-0.1843	254.382	256.882
60	GEV _t -0	56.031	11.731	0.0378	249.737	250.660
	GEV _t -I	43.784 + 0.924t	11.435	-0.1351	243.68	245.280
	GEV _t -II	53.8771	5.053 + 0.537t	-0.2244	245.939	247.539
	GEV _t -III	47.371 + 0.701t	6.122 + 0.329t	-0.1842	241.51	244.010
120	GEV _t -0	32.8	6.997	0.0357	218.655	219.578
	GEV _t -I	25.502 + 0.550t	6.807	-0.136	212.579	214.179
	GEV _t -II	31.512	2.999 + 0.321t	-0.2257	214.801	216.401
	GEV _t -III	27.648 + 0.417t	3.644 + 0.196t	-0.1861	210.397	212.897
360	GEV _t -0	14.102	3.072	0.038	169.36	170.283
	GEV _t -I	10.907 + 0.241t	2.994	-0.1348	163.357	164.957
	GEV _t -II	13.538	1.318 + 0.140t	-0.2201	165.515	167.115
	GEV _t -III	11.849 + 0.182t	1.596 + 0.087t	-0.1826	161.153	163.653
720	GEV _t -0	8.296	1.822	0.0381	138.021	138.944
	GEV _t -I	6.393 + 0.144t	1.768	-0.1326	131.848	133.448
	GEV _t -II	7.955	0.777 + 0.084t	-0.2279	134.2023	135.802
	GEV _t -III	6.940 + 0.110t	0.947 + 0.051t	-0.1856	129.6695	132.170
1440	GEV _t -0	4.8917	1.08	0.0462	106.897	107.820
	GEV _t -I	3.783 + 0.084t	1.058	-0.1293	101.153	102.753
	GEV _t -II	4.7029	0.476 + 0.049t	-0.216	103.3	104.900
	GEV _t -III	4.100 + 0.064t	0.570 + 0.030t	-0.1764	98.997	101.497

Table 4. GEV distribution fitted stationary IDF curve computed rainfall intensities.

Duration (mins)	Return Period					
	2	5	10	25	50	100
15	177.34	216.17	242.78	277.47	304.00	331.02
30	103.30	126.42	142.28	162.96	178.79	194.91
45	75.41	92.49	104.20	119.47	131.15	143.06
60	60.36	74.14	83.59	95.92	105.35	114.97
120	35.38	43.58	49.20	56.51	62.09	67.78
360	15.24	18.84	21.32	24.55	27.03	29.55
720	8.97	11.11	12.58	14.50	15.96	17.46
1440	5.29	6.57	7.45	8.61	9.51	10.43

Table 5. GEV distribution fitted non-stationary IDF curve computed rainfall intensities.

Duration (mins)	Return Period					
	2	5	10	25	50	100
15	216.03	259.09	283.02	308.87	325.33	339.67
30	126.31	151.96	166.22	181.64	191.46	200.03
45	92.43	111.36	121.88	133.26	140.51	146.83
60	74.07	89.35	97.85	107.04	112.89	118.00
120	43.54	52.64	57.69	63.15	66.61	69.63
360	18.81	22.82	25.06	27.48	29.03	30.37
720	11.11	13.49	14.80	16.23	17.13	17.92
1440	6.55	7.97	8.77	9.63	10.19	10.67

3.1.3. Comparison of Percentage Difference between Non-Stationary and Stationary Computed Rainfall Intensities

A visual perusal of the rainfall intensities distribution in **Figure 3** and **Figure 4** of the various graphical plots against duration and/or return period, respectively, indicates the likely existence of a difference between the non-stationary and the stationary models at each plotting point. Therefore, it is imperative to verify if the differences were indeed significant. Intensities obtained from **Table 4** and **Table 5** for stationary and non-stationary, respectively were computed to obtain their percentage differences in the predicted intensities.

In order to verify if the percentage differences were really significant at a 95% confidence level, the Wilcoxon non-parametric paired test of significance was applied to verify this fact. Thus, the two-tailed statistic test was performed for rainfall intensities versus duration for given return period as presented in **Table 6** and for rainfall intensities against the return period for the given duration as presented in **Table 7**. The Wilcoxon test statistic was computed and compared against the critical p-value at alpha, α -value of 5% level of significance.

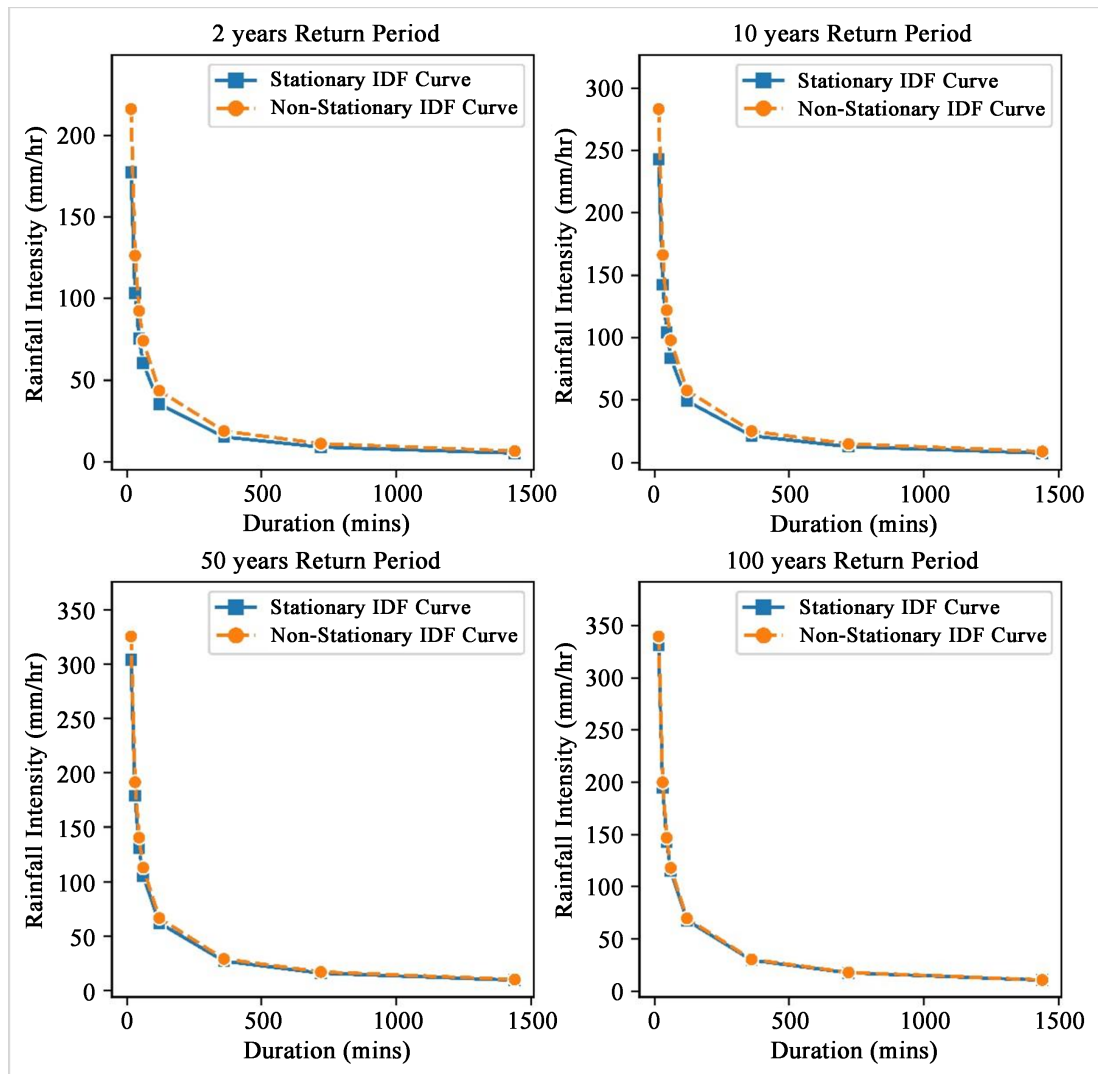


Figure 3. GEV distribution fitted stationary versus non-stationary IDF curves considering different return periods.

3.2. Discussion of Results

3.2.1. Analysis of Downscaled 24-Hourly AMS Data into Shorter Durations

The analyses of this study were based on 24-hourly historical annual maximum time series data (January to December water year). **Table 2** was constructed by using the Modified Chowdhury Indian Meteorological Department (MCIMD) downscaling method given in Equation (4). The calibrated equation produced higher rainfall intensities than the IMD method of Equation (1) for different shorter durations of 0.25 to 1.0 hours applicable for typical urban drainage designs, and 2 to 24 hours longer duration applicable for rural or large scale infrastructural design. The plotting of the rainfall intensities downscaled in mm/hr against duration in years showed a strong increasing (positive) trend from 1985 to 2015 as shown in **Figure 3** for 0.25-hour and 24-hour duration, respectively.

3.2.2. Analysis of GEV Distribution Fitted Non-Stationary IDF Curves

The R-studio software was adopted for all the computations made to obtain the rainfall IDF curves fitted on the basis of GEV distribution. The basic equation

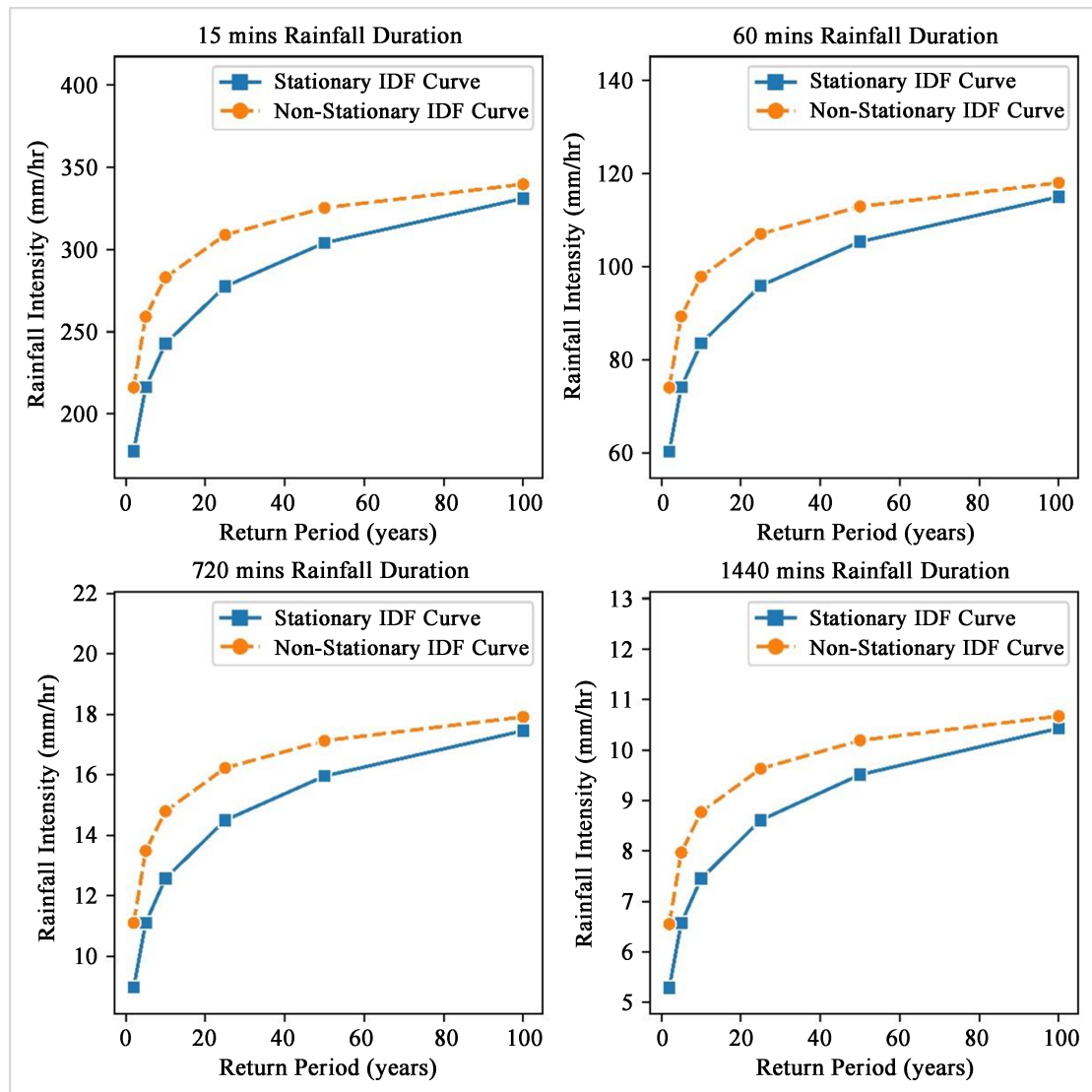


Figure 4. GEV distribution fitted stationary versus non-stationary IDF curves considering different durations.

Table 6. Wilcoxon paired sample test of significant for rainfall intensity for various return period.

Statistical Parameters	Return Period (years)					
	2	5	10	25	50	100
V	0	0	0	0	0	0
Expected Value	18.0000	18.0000	18.0000	18.0000	18.0000	18.0000
Variance (V)	51.0000	51.0000	51.0000	51.0000	51.0000	51.0000
p-value (Two-tailed)	0.0143	0.0143	0.0143	0.0143	0.0143	0.0143

Note: Level of significance @ 5%.

Table 7. Wilcoxon paired sample test of significant for rainfall intensity for various duration.

Statistical Parameters	Duration (mins)							
	15	30	45	60	120	360	720	1440
V	0	0	0	0	0	0	0	0
Expected Value	10.5000	10.5000	10.5000	10.5000	10.5000	10.5000	10.5000	10.5000
Variance (V)	22.7500	22.7500	22.7500	22.7500	22.7500	22.7500	22.7500	22.7500
p-value (Two-tailed)	0.0360	0.0360	0.0360	0.0360	0.0360	0.0360	0.0360	0.0360

Note: Level of significance @ 5%.

which provided the formula for obtaining the cumulative distribution function for the GEV distribution has a family of three distribution functions controlled by the shape function when it is either zero, greater than zero or less than zero given by Equation (5). The expression of the equation into its log-likelihood provided the basis for computing the parameters of the GEV distribution function for both stationary and vis-a-vis the extension of the principles to the non-stationary condition when time is integrated as a co-variate. The parameters were, therefore, computed by optimization which required the minimization of the negative log-likelihood achieved by an iterative process.

Four different linear models integrating time as co-variate were selected as can be seen in **Table 1** and **Table 3** for computation of the GEV distribution function parameters. The first model, GEV_t-0 applies at constant values of location, scale and shape parameters which is also equivalent to the stationary assumption of the GEVT-1. The second model, GEV_t-I have time as a co-variate with location as a parameter while scale and shape parameters were kept constant. The third model, GEV_t-II has time as a covariate with the scale parameter, while location and shape parameters were also kept constant. The fourth model, GEV_t-III has only the shape parameter kept constant while time serves as a co-variate with both locations and scale parameters.

3.2.3. Analysis of Selection Process for Best Parameter Model

From the foregoing, it was ideal to select the best-performing linear model. The statistical method was based on Corrected Akaike Information Criteria (AIC_C) processed by applying Equations (12) to (14). The model with the least AIC_C is considered a reasonable and good choice. From **Table 3**, the GEVt-III which had time as co-variables with both location and scale parameters while the shape parameter was kept constant gave the least AIC_C for all durations analyzed. Thus, the fourth model, GEVt-III, was selected as the best parameter model, used for the computation of the non-stationary rainfall intensities for the different return periods of 2, 5, 10, 25, 50, and 100 years.

Furthermore, to compute the intensity levels for various downscaled durations for any given return period Equation (5) was inverted to derive Equation (16) used.

Also, the values of the best linear parameter model were substituted accordingly to obtain **Table 5**, while **Table 4** intensities were obtained based on model 1, GEVt-0, which is equivalent to the stationary assumption. However, the intensities of **Table 4** and **Table 5**, which were for Stationary and Non-stationary IDF curves, differed glaringly.

3.2.4. Comparative Analysis of Non-Stationary and Stationary IDF Curve Distributions

Rainfall intensity levels computed for stationary and non-stationary fitted distributions shown in **Table 4** and **Table 5**, respectively, were plotted together in a normal graph paper against various durations for given return periods as shown in **Figure 3**. Also, for given durations, both intensities were plotted against the return period as indicated in **Figure 4**. In both plots remarkable differences were observed in the intensity values distribution with the non-stationary intensity distribution giving higher values above those of stationary distributions proving that for the Niger Delta region, the stationary assumption delivers IDF curves that underestimate extreme events as in literature [3] [4] [28]. The implication, therefore, means that if the stationary IDF curve values were applied for infrastructural design such a project may not guarantee safety against more extreme hydrologic events as indicated by the non-stationary counterpart for any particular return period. For instance, for a 2-year return period event, a 1-hr storm duration gave the difference between the non-stationary (74.07 mm/hr) and stationary (60.36 mm/hr), the extreme rainfall of about 13.71 mm/hr (+22.71%). Also, for a 10-year return period event, the 1-hr storm event produced for non-stationary (97.85 mm/hr) and stationary (83.59 mm/hr) giving the extreme rainfall difference of 14.26 mm/hr (+17.0%). The differences of 13.71 mm/hr to 14.26 mm/hr in rainfall intensity especially for small catchment areas could lead to serious underestimation of the peak flood from a stationary IDF curve. This extreme value could further exacerbate the flood risk greater than the provided design of such drainage infrastructure. These findings were consistent with the publication of [3].

Also, observed is that the differences occurring between the non-stationary and stationary intensities increased with higher durations from 15 to 720 min, but reduced in value at 1440 min. This is indicative that longer-duration events have not changed significantly over the succeeding years in the time series, while shorter-duration events intensified increasingly as postulated by [3].

Further investigation of storm durations revealed that the differences between non-stationary and stationary were larger at short durations. For instance, at a 2-year return period, the difference between the IDF curves reduced from 13.71 mm/hr to 2.13 mm/hr for 1-hour and 12-hour storm durations, respectively. While for the 100-year return period, the difference at 1 hour is 3.03 mm/hr which reduction tends to zero (about 0.46 mm/hr) at 12-hour storm duration. This result by implication calls for more focus on the emphasis of considering shorter duration storm for design purposes because it is not only occurring with

higher intensities but also shows evidence of higher differences in the extreme values between the non-stationary and stationary IDF predicted intensities which has the potential of increasing the flood risk and consequential infrastructural failures.

The conduct of performance evaluation for a two-tailed sample using Wilcoxon signed rank sum statistic to further establish the existence of statistical significance difference between the intensities of non-stationary and stationary IDF predicted intensities was carried out. The performance evaluation was carried out for given return periods as presented in **Table 6** and also for the given duration as presented in **Table 7**. The Wilcoxon signed rank sum test statistic calculated is 0.0143 for all return periods, which is less than the critical p-value at alpha, $\alpha = 0.05$. Similarly, the second test showed the Wilcoxon signed rank sum test statistic was calculated as 0.0360 for all durations. These values are less than the critical p-value at a 5% level of significance. The result proves that there is a significant statistical difference between the non-stationary and stationary IDF rainfall intensity distribution.

4. Conclusions

For the computation of intensity levels for the non-stationary IDF models, the best parameter model among four linear parameter models integrating time as co-variate obtained using the Corrected Akaike Information Criteria (AIC_C) showed the fourth model, GEV_t -III that had time as co-variates with both location and scale parameter, with the shape parameter kept constant was selected as the best parameter model because it produced the least AIC_C for all durations.

Intensity levels computed for stationary and non-stationary predicted intensities showed that the non-stationary intensities gave higher values above those of stationary, proving that the stationary assumption IDF curves underestimates extreme events. The differences of 13.71 mm/hr (22.71%) to 14.26 mm/hr (17.0%) in rainfall intensity especially for small watersheds could lead to serious underestimation of the peak flood from a stationary IDF model. The extreme values could further exacerbate the flood risk greater than the provided design for such drainage infrastructure. Wilcoxon paired signed rank sum test statistics for the rainfall intensities for various durations or return periods were examined. The result proves that there is a significant difference between the non-stationary and stationary IDF rainfall intensity distributions to further provide glaring evidence of the existence of an increase in extreme events inducing a climatic change in the study region.

Also, the differences between the non-stationary and stationary intensities increased with higher durations from 15 to 720 min, but reduced in value at 1440 min is indicative that shorter duration events intensified increasingly while longer duration events have not changed significantly over the decades. Consequently, emphasis should be on shorter-duration storms for design purposes because it is not only producing higher intensities, but also showed evidence of higher differ-

ences in the extreme values which have the potential of increasing the flood risk and resultant infrastructural failures.

Conflicts of Interest

The authors declare no conflicts of interest regarding the publication of this paper.

References

- [1] Ouarda, T.B.M.J., Yousef, L.A. and Charron, C. (2019) Non-Stationary Intensity-Duration-Frequency Curves Integrating Information Concerning Teleconnections and Climate Change. *International Journal of Climatology*, **39**, 2306-2323. <https://doi.org/10.1002/joc.5953>
- [2] Adamowski, K. and Bougadis, J. (2006) Detection of Trends in Annual Extreme Rainfall. *Hydrological Processes*, **17**, 3547-3560. <https://doi.org/10.1002/hyp.1353>
- [3] Cheng, L. and AghaKouchak, A. (2014) Nonstationarity Precipitation Intensity-Duration-Frequency Curves for Infrastructure Design in a Changing Climate. *Science Reports*, **4**, Article No. 7093. <https://doi.org/10.1038/srep07093>
- [4] Ganguli, P. and Coulibaly, P. (2017) Does Non-Stationary in Rainfall Require Non-Stationary Intensity-Duration-Frequency Curves? *Hydrology and Earth System Sciences*, **21**, 6461-6483. <https://doi.org/10.5194/hess-21-6461-2017>
- [5] Aghakouchak, A., Ragno, E., Love, C. and Moftakhari, H. (2018) Projected Changes in California's Precipitation Intensity-Duration-Frequency Curves. California's Fourth Climate Change Assessment, California Energy Commission.
- [6] Ren, H., Hou, Z.J., Wigmosta, M., Liu, Y. and Leung, L.R. (2019) Impacts of Spatial Heterogeneity and Temporal Non-Stationarity of Intensity-Duration-Frequency Estimates—A Case Study in a Mountainous California-Nevada Watershed. *Water*, **11**, Article 1296. <https://doi.org/10.3390/w11061296>
- [7] Okon, K.E., Oworen, U., Daniel, K.S. and Okon, I.K. (2019) Occupational Hazard and Work Safety among Chainsaw Operators in Nigeria. *Environment*, **3**, 8-20.
- [8] Udosen, C.E. (2012) Rainfall Trends in Uyo-Akwa Ibom State and Its Implication on Urban Flooding. *Journal of Engineering and Applied Sciences*, **7**, 79-85. <https://doi.org/10.3923/jeasci.2012.79.85>
- [9] Ramaseshan, S. (1996) Urban Hydrology in Different Climate Conditions. Lecture Notes of the International Course on Urban Drainage in Developing Countries, Regional Engineering College, Warangal.
- [10] Rashid, M., Faruque, S. and Alam, J. (2012) Modelling of Short Duration Rainfall Intensity Duration Frequency (SDRIDF) Equation for Sylhet City in Bangladesh. *ARPJN Journal of Science and Technology*, **2**, 92-95.
- [11] Nwaogazie, I.L., Sam, M.G. and David, A.O. (2021) Predictive Performance Analysis of PDF-IDF Model Types Using Rainfall Observations from Fourteen Gauged Stations. *International Journal of Environment and Climate Change*, **11**, 125-143. <https://doi.org/10.9734/ijecc/2021/v11i130349>
- [12] Zakwan, M. (2016) Application of Optimization Techniques to Estimate IDF Parameters. Water and Energy Research Digest (Water Resources Section). *Water and Energy International*, 69-71.
- [13] Sam, M.G., Nwaogazie, I.L. and Ikebude, C. (2021) Improving Indian Meteorological Department Method for 24-Hourly Rainfall Downscaling to Shorter Durations

- for IDF Modeling. *International Journal of Hydrology*, **52**, 72-82.
<https://doi.org/10.15406/ijh.2021.05.00268>
- [14] Sam, M.G., Nwaogazie, I.L. and Ikebude, C. (2022) Non-Stationary Trend Change Point Pattern Using 24-Hourly Annual Maximum Series (AMS) Precipitation Data. *Journal of Water Resources and Protection*, **14**, 592-609.
<https://doi.org/10.4236/jwarp.2022.148031>
- [15] Yue, S. and Wang, C. (2004) The Mann-Kendall Test Modified by Effective Sample Size to Detect Trend in Serially Correlated Hydrological Series. *Water Resources Management*, **18**, 201-218. <https://doi.org/10.1023/B:WARM.0000043140.61082.60>
- [16] Ahmad, I., Tango, D., Wang, T., Wang, M. and Wagan, B. (2015) Precipitation Trends over Time Using Mann-Kendall and Spearman's Rho Tests in Swat River Basin, Pakistan. *Advances in Meteorology*, **2015**, Article ID: 431860.
<https://doi.org/10.1155/2015/431860>
- [17] Okafor, G.C., Jimoh, O.D. and Larbi, K.I. (2017) Detecting Changes in Hydro-Climatic Variables during the Last Four Decades (1975-2014) on Downstream Kaduna River Catchment, Nigeria. *Atmospheric and Climate Sciences*, **7**, 161-175.
<https://doi.org/10.4236/acs.2017.72012>
- [18] Cheng, L., AghaKouchak, A., Gilleland, E. and Katz, R.W. (2014) Non-Stationary Extreme Value Analysis in a Changing Climate. *Climate Change*, **127**, 353-369.
<https://doi.org/10.1007/s10584-014-1254-5>
- [19] Overeem, A., Buishand, A. and Holleman, I. (2007) Rainfall Depth-Duration-Frequency Curves and Their Uncertainties. *Journal of Hydrology*, **348**, 124-134.
<https://doi.org/10.1016/j.jhydrol.2007.09.044>
- [20] Millington, N., Das, S. and Simonovic, S.P. (2011) The Comparison of GEV, Log-Pearson Type 3 and Gumbel Distributions in the Upper Thames River Watershed under Global Climate Models. Water Resources Research Report No. 77, Facility for Intelligent Decision Support, Department of Civil and Environmental Engineering, London, 53 p.
- [21] Coles, S., Bawa, J., Trenner, L. and Dorazio, P. (2001) An Introduction to Statistical Modeling of Extreme Values. Springer, London.
<https://doi.org/10.1007/978-1-4471-3675-0>
- [22] Katz, R.W. (2013) Statistical Methods for Nonstationary Extremes. In: AghaKouchak, A., Easterling, D., Hsu, K., Schubert, S. and Sorooshian, S., Eds., *Extremes in a Changing Climate*, Springer, Dordrecht, 15-37.
https://doi.org/10.1007/978-94-007-4479-0_2
- [23] Renard, B., Sun, X. and Lang, M. (2013) Bayesian Methods for Non-Stationary Extreme Value Analysis. In: AghaKouchak, A., Easterling, D., Hsu, K., Schubert, S. and Sorooshian, S., Eds., *Extremes in a Changing Climate*, Springer, Dordrecht, 39-95.
https://doi.org/10.1007/978-94-007-4479-0_3
- [24] Meehl, G.A., *et al.* (2000) An Introduction on Trends in Extreme Weather and Climate Events: Observations, Socioeconomic Impacts Terrestrial Ecological Impacts and Model Projections. *Bulletin of the American Meteorological Society*, **81**, 413-416.
[https://doi.org/10.1175/1520-0477\(2000\)081<0413:AITTIE>2.3.CO;2](https://doi.org/10.1175/1520-0477(2000)081<0413:AITTIE>2.3.CO;2)
- [25] Katz, R. (2010) Statistics of Extremes in Climate Change. *Climate Change*, **100**, 71-76. <https://doi.org/10.1007/s10584-010-9834-5>
- [26] Gilleland, E. and Katz, R.W. (2011) New Software to Analyze How Extremes Change Over Time. *Eos Transactions American Geophysical Union*, **92**, 13-14.
<https://doi.org/10.1029/2011EO020001>
- [27] Gilleland, E. and Katz, R.W. (2016) ExtRemes 2.0: An Extreme Value Analysis Pack-

- age in R. *Journal of Statistical Software*, **72**, 1-39.
<https://doi.org/10.18637/jss.v072.i08>
- [28] Silva, D.F. and Simonovic, S.P. (2020) Development of Nonstationary Rainfall Intensity Duration Frequency Curves for Future Climate Conditions. Water Resources Research Report No. 106, Department of Civil and Environmental Engineering, Western University, London, 43 p.
- [29] El Adlouni, S., Ouarda, T.B.M.J., Zhang, X., Roy, R. and Bobee, B. (2007) Generalized Maximum Likelihood Estimators for the Nonstationary Generalized Extreme Value Model. *Water Resources Research*, **43**, W03410.
<https://doi.org/10.1029/2005WR004545>
- [30] Sugahara, S., Rocha, R.P. and Silveira, R. (2009) Non-Stationary Frequency Analysis of Extreme Daily Rainfall in Sao Paulo, Brazil. *International Journal of Climatology*, **29**, 1339-1349. <https://doi.org/10.1002/joc.1760>
- [31] Cooley, D. (2013) Return Periods and Return Levels under Climate Change. In: AghaKouchak, A., Easterling, D., Hsu, K., Schubert, S. and Sorooshian, S., Eds., *Extremes in a Changing Climate*, Springer, Dordrecht, 97-114.
https://doi.org/10.1007/978-94-007-4479-0_4
- [32] Kothari, C.R. and Garg, G. (2014) *Research Methodology: Methods and Techniques*. 3rd Edition, New Age International Publishers Limited, New Delhi.
- [33] RStudio Team (2020) *RStudio: Integrated Development for R*. RStudio, PBC, Boston, MA URL. <http://www.rstudio.com/>